



Unusual marine cyanobacteria/haptophyte symbiosis relies on N₂ fixation even in N-rich environments

Matthew M. Mills¹ · Kendra A. Turk-Kubo² · Gert L. van Dijken¹ · Britt A. Henke² · Katie Harding² · Samuel T. Wilson³ · Kevin R. Arrigo¹ · Jonathan P. Zehr²

Received: 15 November 2019 / Revised: 11 May 2020 / Accepted: 27 May 2020 / Published online: 10 June 2020
© The Author(s) 2020. This article is published with open access

Abstract

The microbial fixation of N₂ is the largest source of biologically available nitrogen (N) to the oceans. However, it is the most energetically expensive N-acquisition process and is believed inhibited when less energetically expensive forms, like dissolved inorganic N (DIN), are available. Curiously, the cosmopolitan N₂-fixing UCYN-A/haptophyte symbiosis grows in DIN-replete waters, but the sensitivity of their N₂ fixation to DIN is unknown. We used stable isotope incubations, catalyzed reporter deposition fluorescence in-situ hybridization (CARD-FISH), and nanoscale secondary ion mass spectrometry (nanoSIMS), to investigate the N source used by the haptophyte host and sensitivity of UCYN-A N₂ fixation in DIN-replete waters. We demonstrate that under our experimental conditions, the haptophyte hosts of two UCYN-A sublineages do not assimilate nitrate (NO₃⁻) and meet little of their N demands via ammonium (NH₄⁺) uptake. Instead the UCYN-A/haptophyte symbiosis relies on UCYN-A N₂ fixation to supply large portions of the haptophyte's N requirements, even under DIN-replete conditions. Furthermore, UCYN-A N₂ fixation rates, and haptophyte host carbon fixation rates, were at times stimulated by NO₃⁻ additions in N-limited waters suggesting a link between the activities of the bulk phytoplankton assemblage and the UCYN-A/haptophyte symbiosis. The results suggest N₂ fixation may be an evolutionarily viable strategy for diazotroph–eukaryote symbioses, even in N-rich coastal or high latitude waters.

Introduction

Primary production by marine phytoplankton is limited by N availability throughout much of the global open oceans [1].

These authors contributed equally: Matthew M. Mills, Kendra A. Turk-Kubo

Supplementary information The online version of this article (<https://doi.org/10.1038/s41396-020-0691-6>) contains supplementary material, which is available to authorized users.

✉ Matthew M. Mills
mmmills@stanford.edu

✉ Kendra A. Turk-Kubo
kturk@ucsc.edu

¹ Earth System Science, Stanford University, Stanford, CA 94305, USA

² Ocean Science Department, University of California at Santa Cruz, Santa Cruz, CA 95064, USA

³ Center for Microbial Oceanography: Research and Education, University of Hawaii at Manoa, Honolulu, HI 96822, USA

As a result, phytoplankton have evolved metabolisms for utilizing different chemical forms of N (e.g., NO₃⁻, ammonium (NH₄⁺), or urea; [2]). One important N source for oligotrophic waters is N₂ fixation, the conversion of N₂ into biologically available ammonia, performed by some prokaryotes (diazotrophs), but no eukaryotes. Marine N₂ fixation was once thought to be dominated by the tropical/subtropical cyanobacterium *Trichodesmium* sp. and cyanobacterial symbionts of some diatoms [3, 4]. This paradigm changed with the discovery that N₂ fixation is also carried out by the unicellular N₂-fixing cyanobacterial “group A” (UCYN-A; [5]), which lives in symbiosis with single-celled phytoplankton hosts related to the haptophyte *Braarudosphaera bigelowii* [6, 7]. UCYN-A is unusual in that it has a streamlined genome, lacking photosystem II, Rubisco, the Calvin Cycle, the TCA cycle, and NO₃⁻ assimilation pathways [8, 9]. The haptophyte provides photosynthetically fixed C to UCYN-A in exchange for N supplied by UCYN-A from N₂ fixation [7]. Two genetically distinct UCYN-A symbionts, UCYN-A1 and UCYN-A2, have similarly streamlined genomes [9], but are associated with morphologically and physiologically distinct haptophyte hosts [10, 11].

Table 1 Summary of T_0 parameters for NO_3^- and NH_4^+ addition experiments and T_{48} treatment concentrations.

Experiment	Lat, Lon (ddm)	Date	$\text{NO}_3^- + \text{NO}_2^-$ (μM)	NO_2^- (μM)	NH_4^+ (μM)	PO_4^{3-} (μM)	Si (μM)	T ($^\circ\text{C}$)	Treatment T_{48} $\text{NO}_3^- + \text{NO}_2^-$ (μM)	Treatment T_{48} NH_4^+ (μM)
NO3.1	32.84, -117.531	May 3–5, 2017	0	nm	0.29	nm	16.7 ± 0.16	0.14 ± 0.01	0.8	nm
NO3.2	28.289, -115.914	Oct 6–8, 2017	nm	nm	0.14	0.17	21.5 ± 0.00	0.07 ± 0.01	1.45 ± 0.03	nm
NO3.3	30.358, -116.359	Oct 7–9, 2017	nm	nm	0.13	3.18	19.3 ± 0.22	0.16 ± 0.02	1.42 ± 0.05	nm
NH4.1	32.867, -117.256	May 10–12, 2018	0.13^a	0.25^a	0.29^a	9.02^a	14.9 ± 0.14^a	3.94 ± 0.42	nm	0.80 ± 0.43

NO3.1 was conducted on the R/V Robert Gordon Sproul in the proximity of the SIO pier in May 2017. NO3.2 and NO3.3 were conducted at stations off the coast of Baja California Sur, Mexico in October 2017. NH4.1 was conducted at the SIO pier in May 2018 (Fig. S1).

nm not measured.

^aFrom SCOOS monitoring data at SIO pier on May 10, 2018.

The fixation of N_2 is energetically expensive, requiring large amounts of ATP and reductant compared with the assimilation of dissolved inorganic nitrogen (DIN) [12]. The sensitivity of marine N_2 fixation to DIN concentrations is not well understood [13]. Culture-based studies show that N_2 fixation by the cyanobacterial diazotroph *Trichodesmium* can be inhibited at elevated DIN concentrations (e.g., [14–16]), but notably growth and N_2 fixation rates in the unicellular *Crocospaera* can be insensitive to DIN availability [17–19]. The biogeography of the UCYN-A/haptophyte symbiosis extends into DIN-replete environments not typically considered important for N_2 fixation, including cold high latitude waters [20, 21], coastal shelves [22, 23], and upwelling regions [24]. Recent evidence suggests that UCYN-A can grow in high NO_3^- waters [25] and that N_2 fixation in UCYN-A may not be completely inhibited by the presence of combined forms of DIN [26]. However, it is still not well understood whether growth of the UCYN-A/haptophyte symbiosis is supplemented by a N source other than UCYN-A N_2 fixation when DIN is available to the haptophyte.

To determine the N source(s) used for growth by the UCYN-A1/ and UCYN-A2/haptophyte symbioses, we conducted a series of experiments in the southern coastal waters of the California Current System (CCS; Table 1). A fully replicated design (details below) was implemented to assess the effects of NO_3^- or NH_4^+ additions on bulk community responses (chlorophyll *a* (Chl *a*) and particulate organic carbon (POC) and nitrogen (PON) concentrations), as well as N_2 fixation, C fixation, and DIN uptake rates by the bulk phytoplankton assemblage and the UCYN-A/haptophyte symbioses specifically. The stable isotope tracers $^{15}\text{N}_2$, $^{15}\text{NO}_3^-$, $^{15}\text{NH}_4^+$ and $\text{H}^{13}\text{CO}_3^-$ were used to measure N_2 fixation, DIN uptake, and C fixation rates, respectively, by the phytoplankton assemblage. The cell-specific UCYN-A/haptophyte symbioses were measured using sublineage-specific catalyzed reporter deposition fluorescence in-situ hybridization (CARD-FISH) assays [27, 28] combined with nanoscale secondary ion mass spectrometry (nanoSIMS). The experiments were designed to investigate whether UCYN-A continues to fix N_2 when NO_3^- and NH_4^+ are readily available, if the haptophyte host takes up NO_3^- and

NH_4^+ , and if responses to $\text{NO}_3^-/\text{NH}_4^+$ additions were UCYN-A/haptophyte sublineage-specific.

Materials and methods

DIN experiments: experimental design and sampling

Four experimental manipulations were conducted during 2017 and 2018 in the southern coastal waters of the CCS; three experiments (NO3.1, NO3.2, NO3.3) were NO_3^- addition experiments and one was an NH_4^+ addition experiment (NH4.1). NO3.1–3 were conducted at three different stations aboard the R/V Gordon Sproul during two research cruises in 2017 that transited off the coast of Southern California and Baja California Sur, Mexico, while NH4.1 was conducted on the Scripps Institute of Oceanography pier (Table 1, Fig. S1).

For NO3.1–3, surface water was pumped into 40 L carboys, housed in an on-deck laboratory container, using a pneumatic (PVDF and Teflon) diaphragm pump (Wilden Pump and Engineering, Grand Terrace, CA), to allow mixing of the seawater before being randomly dispensed into acid-cleaned 4 L polycarbonate bottles (Thermo Scientific™ Nalgene™, Waltham, MA). Grazers were removed using 150 μm Nitex™ plankton netting (BioQuip, Rancho Dominguez, CA). The bottles were then incubated in triplicate with or without an addition of NO_3^- ($2 \mu\text{mol L}^{-1}$ final concentration) at T_0 , according to the experimental design in Fig. S2. Incubation bottles were placed in a flow-through surface seawater incubator, amended with neutral density screening to attenuate incident light to 20% of the surface irradiance. Incubations lasted 48 h, with initial rate measurements between 0 and 24 h and final rate measurements between 24 and 48 h. Final concentrations of ^{15}N - and ^{13}C -labeled substrates for rate measurements are detailed in Table S2. At each time point, bottles were sacrificed and subsampled for measuring Chl *a* concentration, dissolved and particulate nutrient concentrations, bulk CO_2 and N_2 fixation rates, inorganic N uptake rates, flow cytometry, diazotroph abundance (qPCR-based estimates using assays

targeting the *nifH* gene), and UCYN-A/haptophyte symbiosis cell-specific N₂ fixation, CO₂ fixation and NO₃⁻ uptake rates (CARD-FISH, nanoSIMS). Unlabeled initial samples were used to determine the atom% ¹⁵N- and ¹³C-normal of the unenriched bulk community and UCYN-A/haptophyte symbioses.

For NH₄.1, surface water was pumped into 40 L carboys from the waters surrounding the SIO Pier using a pneumatic (PVFD and Teflon) diaphragm pump (Wilden Pump and Engineering), then randomly dispensed into acid-cleaned 2 L polycarbonate bottles (Thermo Scientific™ Nalgene™). Grazers were removed using 150 μm Nitex™ plankton netting (BioQuip, Rancho Dominguez, CA). The bottles were then incubated with or without an NH₄⁺ addition (2 μmol L⁻¹ final concentration) at T₀, according to the experimental design in Fig. S3. Incubation bottles were placed in a flow-through surface seawater incubator, amended with neutral screening to attenuate incident light to 20% of the surface irradiance. Incubations lasted 48 h, with N₂ fixation initial rate measurements between 0 and 24 h and final rate measurements between 24 and 48 h. For NH₄⁺ uptake rates, initial rates were measured between 0 and 6 h, and final rates in NH₄⁺-treatments were measured between 45 and 51 h. Incubation times (6 h) were chosen to ensure detection of isotope enrichments while minimizing isotope dilution, as recommended in Glibert [29]. Final concentrations of ¹⁵N-labeled substrates for rate measurements are detailed in Table S2. At each time point, bottles were sacrificed and subsampled for Chl *a* concentration, dissolved and particulate nutrient concentrations, bulk CO₂ and N₂ fixation rates, inorganic N uptake rates, diazotroph abundance (DNA), and UCYN-A/haptophyte symbiosis cell-specific N₂ fixation, CO₂ fixation, and NO₃⁻ uptake rates (CARD-FISH, nanoSIMS). Unlabeled initial samples were used to determine the atom% ¹⁵N- and ¹³C-normal of the unenriched bulk community and UCYN-A/haptophyte symbioses.

Dissolved and particulate nutrient analyses

Samples for the measurement of NO₃⁻ + NO₂⁻, PO₄³⁻, and Si(OH)₄ concentrations were filtered through precombusted (450 °C for 4.5 h) 25 mm GF/F filters and stored in acid-cleaned Falcon™ tubes (Thermo Fisher Scientific) at -20 °C until analysis using standard techniques [30] on a Lachat QuikChem 8000 Flow Injection Analyzer. Samples for the analysis of POC and PON were filtered onto precombusted (4 h @ 450 °C) 25 mm Whatman GF/F filters. Blank filters were made by filtering ca. 25 ml filtered (0.2 μm) seawater and were processed the same as the particulate samples. The filters were dried (60 °C) and stored at room temperature until analysis. Prior to analysis the samples were fumed with concentrated HCl, dried at 60 °C for 24 h,

packed into tin capsules (Costech Analytical Technologies Inc. Valencia, CA) and analyzed on an Elemental Combustion System (Costech Analytical Technologies) interfaced to a Thermo Finnigan Delta V Advantage isotope ratio mass spectrometer (Thermo Fisher Scientific) at the SOEST Biogeochemical Stable Isotope Facility at the University of Hawai'i, Manoa. Fluorometric analysis of Chl *a* was measured [31] using a Turner Fluorometer TD-700 (Turner Designs, Inc., San Jose, CA).

¹⁵N₂ fixation and C fixation rate measurements

We measured ¹⁵N₂ incorporation into biomass using a “dissolution approach” amended from Mohr et al. [32] and Wilson et al. [33]. ¹⁵N₂-enriched seawater was generated in batches for each experiment by filtering seawater collected from the experimental site through a Pall 0.2 μm Acropak 1550 Capsule Filter with Supor Membrane (Pall Corp, Port Washington, New York). The filtered seawater (FSW) was degassed under vacuum for 30–60 min, while being stirred. Degassed water was quickly transferred via siphon into 2 or 4 L polycarbonate bottles and capped with PTFE-lined (Ace Glass Incorporated, Vineland, NJ) septa and caps. Bottles were then overpressurized by injecting between 20 and 30 mL of ¹⁵N₂ gas (Cambridge Isotope Laboratories, Tewksbury, MA) and agitated at room temperature on a rocking plate (NH4.1) or by the motion of the ship (NO3.1–NO3.2) for >12 h. To verify the atom% enrichment of each batch of ¹⁵N₂ tracer-labeled seawater, duplicate 12 ml Exetainers® (Labco, Lampeter, Ceredigion, U.K) were filled immediately prior to the initiation of each experimental incubation for subsequent membrane inlet mass spectrometer (MIMS) analysis at the University of Hawai'i at Manoa according to Wilson et al. [33]. The quantity of nitrogen isotopes (i.e., N masses equivalent to 28, 29, and 30) was measured in each batch of ¹⁵N₂ enriched seawater. Calibration of the MIMS was achieved by the analysis of a 1 L reservoir of air-equilibrated filtered (0.2 μm) seawater with a known salinity and a temperature of 23 °C [34]. The final atom% enrichment in the seawater incubations averaged 5.9 ± 1.7 (with a total range of 2.4–8.6 atom% enrichment).

Incubation bottles received 400 mL (NO3.1–NO3.3) or 200 mL (NH4.1) of ¹⁵N₂-enriched FSW to initiate the experiment. Each incubation bottle also received NaH¹³CO₃ (Cambridge isotopes) according to Table S2. Following a 24 h incubation period, samples were gently vacuum filtered onto a combusted 25 mm glass fiber filter and stored at -20 °C until preparation for analysis. Samples were dried, acidified, and prepared for analysis as the POC/PON samples above. The ¹⁵N₂ and ¹³CO₂ enrichment of the particulate material was measured using an Elemental Combustion System CHNS-O (ECS 4010) (Costech Analytical Technologies, Inc. Valencia, CA) interfaced to a

Thermo Scientific Delta V Advantage isotope ratio mass spectrometer at the SOEST Biogeochemical Stable Isotope Facility at the University of Hawai'i at Manoa. LOD, estimates of error and minimum quantifiable rates (MQR) were calculated as in Gradoville et al. [35], and are detailed in Tables S13 and S14.

$^{15}\text{NO}_3^-$ and $^{15}\text{NH}_4^+$ uptake bulk community rate measurements

^{15}N incorporation into biomass from DIN substrates (NO_3^- and NH_4^+) was measured in both control and treatment incubations. ^{15}N substrate additions ($^{15}\text{NO}_3^-$ or $^{15}\text{NH}_4^+$; Cambridge Isotope Laboratories) were made with the goal of enriching the ambient pool ~4–10% (Table S2). For the NO_3^- -addition experiments, ambient NO_3^- concentrations were estimated using NO_3^- -temperature relationships for California Current waters [36], while for NH_4^+ , ambient NH_4^+ concentrations were estimated based on historical data from the Southern California Coastal Ocean Observing System (SCCOOS). Incubation bottles receiving $^{15}\text{NO}_3^-$ or $^{15}\text{NH}_4^+$ also received $\text{NaH}^{13}\text{CO}_3$ (Cambridge Isotope Laboratories) according to Table S2. Following a 24 h incubation period for NO_3^- and a 6 h incubation period for NH_4^+ , samples were gently vacuum filtered onto a precombusted 25 mm glass fiber filter and stored at -20°C until preparation and analysis as described above for the N_2 fixation measurements.

Actual ambient concentrations were typically lower than estimates made using this approach. In cases where ambient NO_3^- concentrations were below detection limits ($\text{LOD} = 0.1 \mu\text{mol L}^{-1}$), substrate pool enrichments were calculated using the LOD [29], and should be considered maximum uptake rates. Ambient NH_4^+ concentrations were measured as part of the SCCOOS monitoring program and isotope enrichments were calculated from these measurements.

Potential isotope dilution effects that may result from NH_4^+ regeneration during NH_4^+ were calculated using regeneration rates measured in Southern California Bight waters by Bronk and Ward [37] (Table S3). Dilution of the NO_3^- isotope pool was not likely to be significant as surface water rates of nitrification in Southern California current waters are typically very low [37].

Phytoplankton uptake of NO_3^- and NH_4^+ are associated with strong isotopic fractionation effects that can lead to the accumulation of an isotopically heavy DIN pool [38]. Assimilation of this isotopically heavy DIN during a $^{15}\text{N}_2$ fixation incubation leads to an overestimation of N_2 fixation rates, or even a false positive for N_2 fixation. This effect is likely insignificant in oligotrophic waters, but not in nutrient rich waters that are transiently poor in nutrients due to phytoplankton consumption. These were the conditions during NH_4^+ , where concentrations of NO_3^- were

$0.46 \mu\text{mol L}^{-1}$ at the time of the experiment but were $6 \mu\text{mol L}^{-1}$ 10 days prior to beginning the experiment. However, we detected no ^{15}N enrichment of the PON pool in the $^{15}\text{N}_2$ incubations and were thus unable to calculate bulk N_2 fixation rates (Fig. 1d, Table S4). As such we do not consider isotopic fractionation of the DIN pool a concern in this experiment. All other experiments were conducted under nutrient limited conditions, thus ambient DIN pools were unlikely enriched due to isotope fractionation.

Measuring UCYN-A/haptophyte symbioses single-cell rates

Experiments with UCYN-A/haptophyte symbioses present at suitable abundance for nanoSIMS analyses were first identified using qPCR targeting the UCYN-A1 and UCYN-A2 *nifH* gene (Supplemental text, Table S5). All UCYN-A/haptophyte symbioses single-cell rates were measured using CARD-FISH to visualize and target the UCYN-A/haptophyte symbioses coupled to nanoSIMS to measure the incorporation of ^{15}N or ^{13}C into individual associations. Subsamples (95 mL) from each incubation bottle were fixed with 5 mL of sterile filtered 37% formaldehyde (MilliporeSigma), fixed for between 1 and 48 h at 4°C in the dark, and then filtered under low vacuum onto a $0.6 \mu\text{m}$ polycarbonate filter (MilliporeSigma). Filters were air dried and frozen at -80°C until processing.

CARD-FISH

Fluorophore-containing tyramides were deposited into host and symbiont cells, using 5'-horseradish peroxidase (HRP)-labeled oligonucleotide probes (Biomers.net, Inc., Ulm/Donau, Germany) targeting each UCYN-A/haptophyte sublineage, in combination with helper and competitor probes for both symbionts and hosts (Biomers.net), as described in [28] and Table S1. Briefly, cells were attached to filters with 0.1% Ultrapure agarose (Life Technologies, Carlsbad, CA), then permeabilized in a two-step process with lysozyme achromopeptidase (MilliporeSigma) solution. Hybridizations with HRP-labeled probes were carried out in hybridization buffer at 46°C for the host hybridizations and 35°C for the symbiont hybridizations. Unincorporated probe was removed with several wash steps with a buffer preheated to 2°C greater than the hybridization temperature. The tyramide signal amplification (TSA) step deposited fluorophore-containing tyramides in the presence of an amplification buffer and hydrogen peroxide. The haptophyte host was labeled with the Alexa 488 fluorophore (Biomers.net), and the symbiont was labeled with the Cy3 fluorophore (Biomers.net). Post amplification, filters were washed with PBS, hydrogen peroxide was deactivated with 0.01 M HCl, then filters were rinsed with Milli-Q™

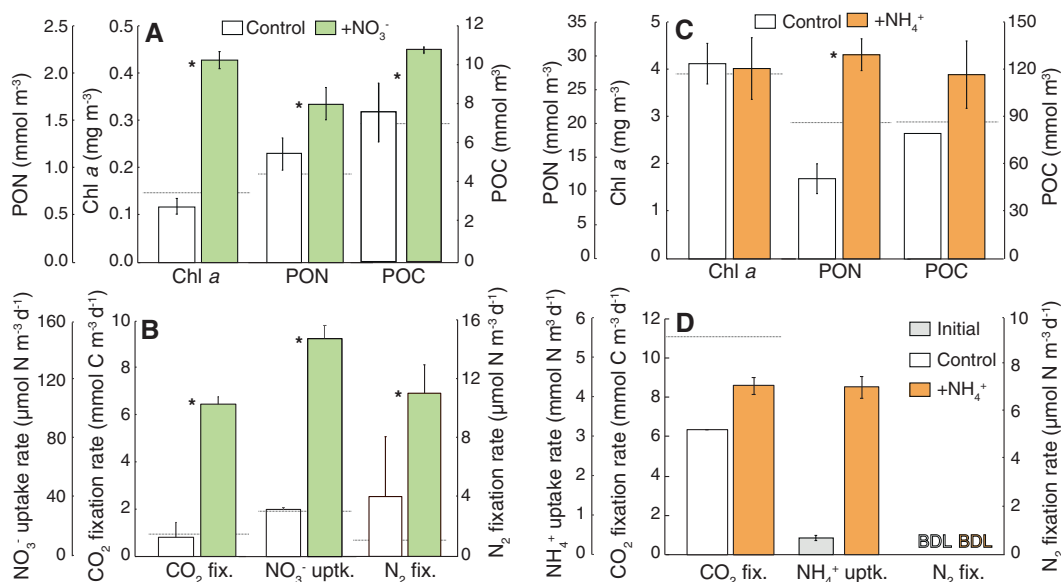


Fig. 1 Bulk particulate and biological rate responses to DIN additions in Southern California Coastal Current Waters. **a, b** Data from NO₃.1 conducted in May 2017. **c, d** Data from NH₄.1 conducted in May 2018. **a** PON, Chl *a* and POC concentrations in control and in 2 μM +NO₃⁻-treatments. **b** Whole community NO₃⁻ uptake rate, CO₂ and N₂ fixation rates in control and in 2 μM +NO₃⁻-treatments. **c** PON, Chl *a* and POC concentrations in control and in 2 μM NH₄⁺-treatments. **d** Whole community NH₄⁺ uptake rate,

CO₂ and N₂ fixation rates in control and in 2 μM +NH₄⁺-treatments. All error bars are standard deviations from biological triplicates. Initial values are denoted with dotted gray lines. BDL indicates measurements below detection and asterisk symbol indicates treatment means are significantly different ($p < 0.05$, $\alpha = 0.05$). Note all bars are time final control and treatment responses, except in (c) where the control NH₄⁺ uptake rate sample was lost and the initial is shown as a gray bar.

(MilliporeSigma) water. After the second round of hybridization, TSA, and washing, filters were dried, and counterstained with ProLong™ Diamond Antifade Mountant with DAPI (Molecular Probes, Eugene, OR).

Filters were visualized on a Zeiss Axioplan epifluorescence microscope (Oberkochen, Germany) equipped with digital imaging to verify that both host and symbiont hybridizations were optimal, allowing for positive identification and mapping of active (vital) UCYN-A/haptophyte symbioses. The filters containing the successfully hybridized cells were then gently rinsed with milli-Q water and then placed cell side down onto an alphanumeric labeled gridded silicon wafer (1.2 × 1.2 cm with a 1 × 1 mm raster, Pelcotec™ SFG12 Finder Grid Substrate, Ted Pella, Redding, CA). The wafer was then placed into a -80 °C freezer for 5–10 min before being removed and the filter peeled off. Particulate matter remaining on the wafer was then allowed to air dry before multiple UCYN-A/haptophyte targets were randomly imaged and mapped at 40x using the above-mentioned epifluorescence microscope.

NanoSIMS analysis and rate calculations

The maps produced from the CARD-FISH imaging were used to locate the UCYN-A/haptophyte targets on a Cameca nanoSIMS 50 L at the Stanford Nano Shared Facilities

(Stanford, CA) using the CCD camera. Symbioses selected for nanoSIMS analysis were randomly selected from the mapped cells for analysis based on ease of localization on the silicon wafer, clarity of the secondary electron image, and magnitude of the ¹²C¹⁴N⁻ signal (i.e., if the image was difficult to focus or if there was sample charging that obscured the signal, a different cell was selected) (Fig. S6). Image fields were then rastered with a 16 keV Cesium primary ion beam (~5 pA). Primary ions were focused into ~120 nm spot diameter and all measurements were made at a mass resolving power of approximately 8000. We rastered an area with 256 × 256 pixels over the chosen raster size with a dwell time of 1 ms per pixel. We collected images of ¹²C⁻, ¹³C⁻, ¹²C¹⁴N⁻ and ¹²C¹⁵N⁻ over 30–100 planes. Both UCYN-A and haptophytes were selected as regions of interest (ROI) using the image analysis software Look@nanoSIMS [39]. Isotope ratios of UCYN-A and the hosts were calculated as the ratio of the sum of total ion counts within the ROIs for each pixel over all recorded planes of the enriched and unenriched isotopes (i.e., ¹³C⁻/¹²C⁻ and ¹²C¹⁵N⁻/¹²C¹⁴N⁻). Corrections for beam and stage drift were made for all scans. Rates were determined as follows:

$$\rho (\text{fmol cell}^{-1} \text{d}^{-1}) = \frac{At\%_{\text{sample}} - At\%_{\text{normal}}}{(At\%_{\text{substrate}} - At\%_{\text{normal}}) \times T} \times B,$$

Where ρ equals the absolute uptake rate per cell, $At\%_{sample}$, $At\%_{normal}$, and $At\%_{substrate}$ equal the atom% ^{15}N or ^{13}C of the enriched (T_{48}) or unenriched (T_0) sample and the respective added ^{15}N or ^{13}C enriched substrate. Substrate enrichments were measured for N_2 following Kana et al. [40] and calculated for DIN and HCO_3^- based on ambient concentrations. In addition, T is time in days and B is the per cell biomass estimates determined from biovolumes as in Krupke et al. [26] and converted to units of N using C:N estimates from Martinez-Perez et al. [11]. Detection limits, estimates of error and MQR were calculated as in Montoya et al. [41] and Gradoville et al. [35] (Tables S13 and S14). N_2 rates, C fixation rates, and $\text{NO}_3^-/\text{NH}_4^+$ uptake rates for both the symbiont and hosts were calculated individually and then summed to get total symbiosis rate for either the symbiont (N_2 fixation) or host (C fixation, $\text{NO}_3^-/\text{NH}_4^+$ uptake). Measuring the isotopic abundance of the symbionts and hosts individually allowed for the inclusion of N transferred from the UCYN-A to the haptophyte and C transferred from the host to the symbiont. Care was taken to measure samples from the same experiments within the same measurement period so as to minimize machine variance between measurement periods.

Statistical analyses

Single factor analysis of variance (ANOVA) was used to evaluate the significance of treatment effects (Control, $+\text{NO}_3^-$, $+\text{NH}_4^+$) on Chl *a* (Table S6), POC (Table S7), PON (Table S8), *nifH*-based UCYN-A abundance (Table S9), and whole community N_2 (Table S10), and C fixation (Table S11), and NO_3^- uptake rates (Table S12). Further ANOVA analyses tested the impact of the NO_3^- and NH_4^+ additions on the single-cell N_2 and C fixation rates in each experiment (Tables S15–22). Treatment responses were considered significantly different at the $\alpha = 0.05$ significance level.

Results

The phytoplankton assemblage response to the addition of NO_3^- indicated they were N-limited throughout the study region. Bulk responses to NO_3^- additions included a 1.7–4.5-fold stimulation of Chl *a* and a 1.3 ± 0.2 and 1.5 ± 0.4 -fold increase in POC and PON concentrations, respectively (Figs. 1a, S4A, B). In addition, bulk C fixation rates, maximum NO_3^- uptake rates, and N_2 fixation rates (in NO3.1) increased up to 13-fold, 9.5-fold, and 4-fold (Figs. 1b, S4C, D), respectively. The diazotroph assemblage at T_0 in NO3.1 included UCYN-A1, UCYN-A2, *Richelia* associated with the diatom *Hemiaulus* and a putative γ -proteobacterial diazotroph, gamma A

(Table S23), each of which may have contributed to bulk N_2 fixation rates. UCYN-A1 abundance was higher in $+\text{NO}_3^-$ treatments than controls at both time points, despite being lower than T_0 abundances (Table S5).

Surprisingly, under these experimental conditions, the haptophyte host of UCYN-A1 did not assimilate NO_3^- (Figs. 2e–h, S5D). The host, however, did exhibit significantly higher C fixation rates in the NO_3^- treatment in NO3.1 ($p < 0.01$; Fig. 2i–l, Table S19) indicating that haptophyte C fixation was indirectly stimulated by the NO_3^- addition. In addition, the average per cell rate of N_2 fixation in the NO_3^- treatment relative to the control in NO3.1 ($p < 0.01$, Fig. 2a–d, Table S15). In general, average N_2 and C fixation per cell rates were higher in NO_3^- treatments, but not always statistically significant (Tables S16 and S20). Notably, the haptophyte host of UCYN-A2 also did not assimilate NO_3^- (Fig. S5D, Table S12).

Since the symbiosis did not assimilate NO_3^- , we also tested for the uptake of NH_4^+ , the most reduced and typically preferred N substrate for phytoplankton [2]. NH_4^+ -addition experiments were conducted in coastal CCS waters (Figs. S1, S3) during the late stages of a bloom of the dinoflagellate *Lingulodinium polyedra*, with relatively high initial DIN concentrations ($0.46 \mu\text{mol L}^{-1} \text{NO}_3^- + \text{NO}_2^-$ and $0.25 \mu\text{mol L}^{-1} \text{NH}_4^+$) and relatively abundant UCYN-A/haptophyte populations (10^4 – 10^5 *nifH* copies L^{-1} ; Table S5). Chl *a* concentrations and bulk C fixation rates were not stimulated by NH_4^+ additions (Fig. 1c, d), but POC/PON concentrations and NH_4^+ uptake rates increased 1.5–2.5- and 5.5-fold, respectively (Fig. 1c, d, Tables S6, S8, S12, Supplemental text). Despite undetectable bulk rates of N_2 fixation (Fig. 1d; Table S4), per cell rates of N_2 and C fixation were measured in both UCYN-A1/ and UCYN-A2/haptophyte symbioses, with no difference in rates between controls and NH_4^+ additions (Fig. 3a, b, e, f, g–j, Tables S13 and S14, Tables S17 and S18, Tables S21 and 22). Surprisingly, NH_4^+ uptake rates were low relative to the N_2 fixation rates in both UCYN-A hosts (Fig. 3c, d, k–n, Table S13), even when accounting for possible isotope dilution effects due to NH_4^+ regeneration (see Methods and Table S3). UCYN-A1 host NH_4^+ uptake rates were not quantifiable (Fig. 3c) while UCYN-A2 host NH_4^+ uptake rates were ~3–10-fold less than measured N_2 fixation rates (Fig. 3d).

Discussion

Our findings indicate that the net benefits of maintaining N_2 fixation must outweigh the costs when compared with the assimilation of DIN for this symbiotic association. N_2 fixation in the UCYN-A/haptophyte symbioses provides N

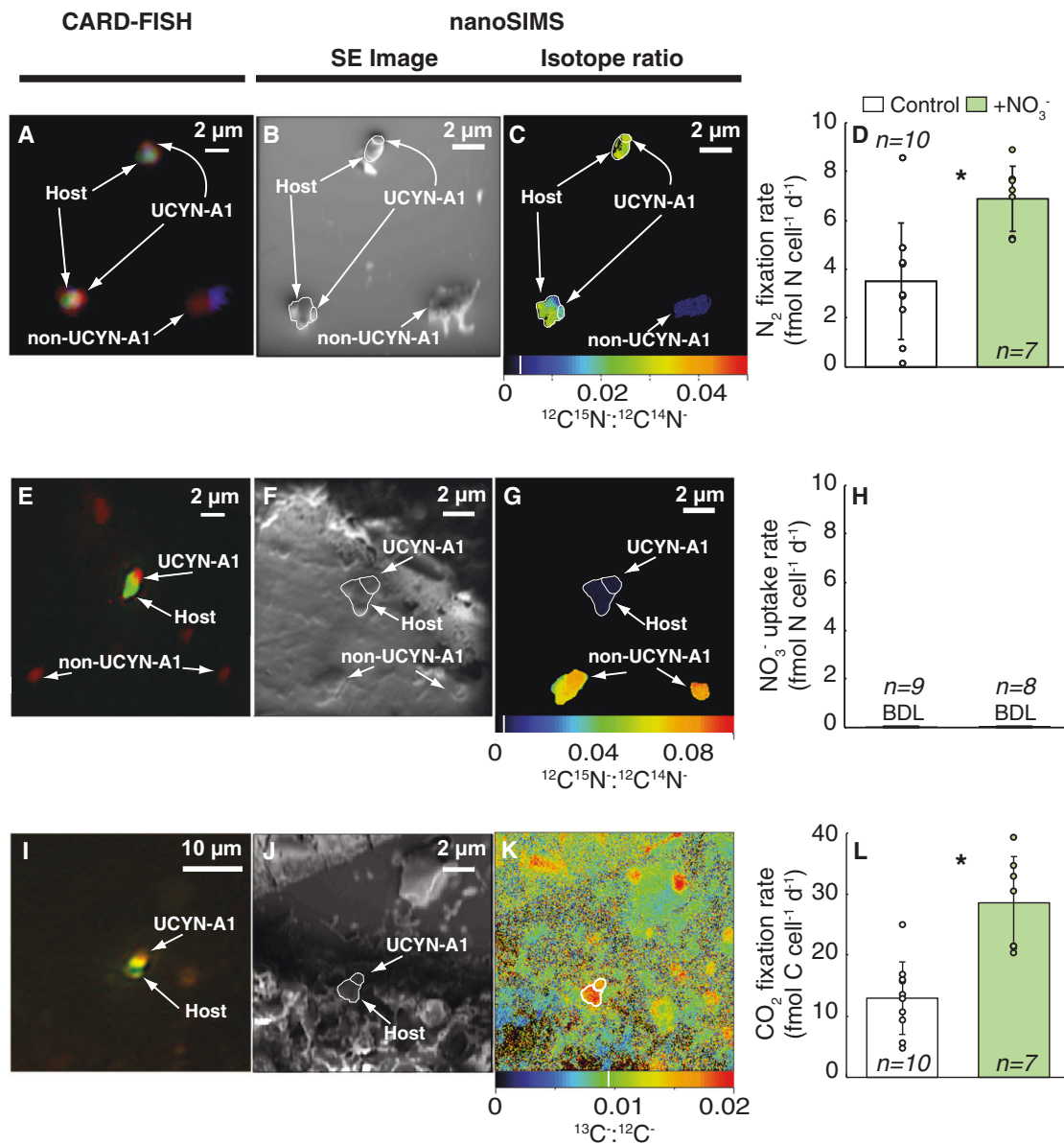


Fig. 2 Individual UCYN-A1/haptophyte cells had higher rates of N₂ and C fixation, but no NO₃⁻ assimilation. Data from NO₃.1; see Fig. S2 for NO₃.2 and NO₃.3. **a–c** Example images of cells from NO₃⁻ treatments, where ¹⁵N enrichment from ¹⁵N₂ fixation was measured. **d** Cell-specific rates of N₂ fixation in control and NO₃⁻ treatments. **e–g** Example images of cells from NO₃⁻ treatments, where ¹⁵N enrichment from ¹⁵NO₃⁻ uptake was measured. **h** Cell-specific rates of NO₃⁻ uptake in control and NO₃⁻ treatments. **i–k** Example images of cells from NO₃⁻ treatments, where ¹³C enrichment from H¹³CO₃⁻ was measured. **l** Cell-specific rates of CO₂ fixation in control and NO₃⁻ treatments. **a, e, i** Epifluorescence micrographs of UCYN-A1 (red) and the haptophyte host (green) stained with

CARD-FISH probes [28] and DAPI (blue). **b, f, j** Corresponding secondary electron (SE) images displaying target cells. Isotope ratio images acquired from nanoSIMS analysis showing isotopic enrichment in ¹⁵N from a ¹⁵N₂ incubation (**c**), ¹⁵N from a ¹⁵NO₃⁻ incubation (**g**), and ¹³C from a H¹³CO₃⁻ incubation (**k**) incubated samples. Data from individual cells (circles) are included in (**d**) and (**l**). Note the difference in scales. Non-UCYN-A1/haptophyte cells are identified for contrast in (**c**) and (**g**). Natural abundances are noted with a white line on the color scale bar in (**c**), (**g**) and (**k**). Rates represent integration over a diel cycle (final 24–48 h). BDL indicates measurements below detection and asterisk symbol indicates treatment means are significantly different ($p < 0.05$, $\alpha = 0.05$).

to the host cell under both N-limited and N-replete conditions, contrary to other marine diazotrophs (e.g., *Trichodesmium*, *Crocospaera*, and the heterocyst-forming symbiont *Richelia* associated with *Rhizosolenia*) for which NO₃⁻ and NH₄⁺ utilization can meet significant proportions of their N requirements when available [14, 15, 17, 18, 42].

The lack of NO₃⁻ assimilation in a eukaryotic alga is highly unusual. In addition, the low rates of NH₄⁺ assimilation by the haptophyte host are also unusual, but could result from high intracellular NH₃ concentrations, due to UCYN-A N₂ fixation, which may create a gradient that prevents uptake [43]. Marine phytoplankton typically

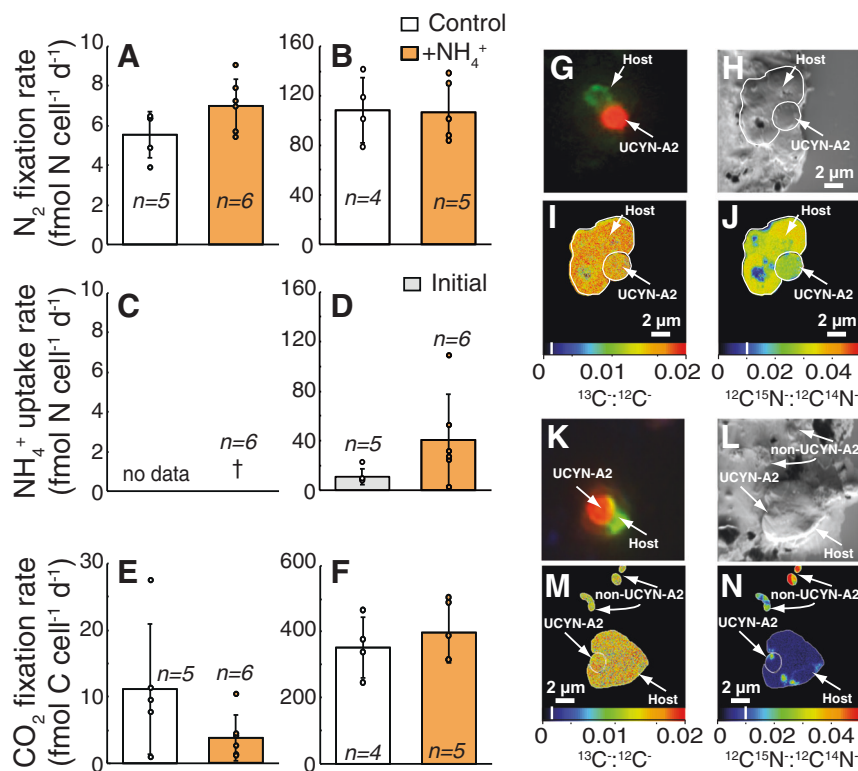


Fig. 3 N₂ fixation in UCYN-A1/ and UCYN-A2/haptophyte symbioses is not inhibited in the presence of NH₄⁺. Cell-specific N₂ fixation rates for the UCYN-A1/haptophyte symbiosis (a) and UCYN-A2/haptophyte symbiosis (b) in control and +NH₄⁺-treatments from NH₄.1. Cell-specific NH₄⁺ uptake rates for the UCYN-A1/haptophyte symbiosis (c) and UCYN-A2/haptophyte symbiosis (d) in control and +NH₄⁺-treatments. Cell-specific CO₂ fixation rates for the UCYN-A1/haptophyte symbiosis (e) and UCYN-A2/haptophyte symbiosis (f) in control and +NH₄⁺-treatments. g–j Example images of a UCYN-A2/haptophyte symbiosis from NH₄⁺-treatments, where ¹⁵N enrichment from ¹⁵N₂ fixation was measured. k–n Example images of a UCYN-A2/haptophyte symbiosis from NH₄⁺-treatments, where ¹⁵N enrichment from ¹⁵NH₄⁺ uptake was measured. g, k Epifluorescence

micrographs of UCYN-A2 (red) and the haptophyte host (green) stained with CARD-FISH probes [28] and DAPI (blue). h, i Corresponding secondary electron (SE) images displaying target cells. Isotope ratio images acquired from nanoSIMS analysis showing isotopic enrichment in ¹³C from a H¹³CO₃⁻ incubation (i, m), ¹⁵N from a ¹⁵N₂ incubation (j), and ¹⁵N from a ¹⁵NH₄⁺ incubation (n). Non-UCYN-A2/haptophyte cells are identified for contrast in (l–m). Data from individual cells (circles) are included in (a–f). N₂ fixation rates represent integration over a diel cycle (final 24–48 h); while NH₄⁺ uptake rates were measured over a 6-h period. Note treatment responses are compared to initials in (d). The Dagger symbol indicates below minimum quantifiable rate. Natural abundances are noted with a white line on the color scale bar in (i), (j), (m), and (n).

possess the metabolic capabilities to assimilate NO₃⁻, although uptake rates and internal storage capabilities vary between species [44]. NO₃⁻ assimilation is common in other haptophyte lineages, including *Emiliania huxleyi* [45] and *Prymnesium parvum* [46]; however nothing is known about the N utilization strategies in *B. bigelowii* beyond N acquisition from the symbiont [7]. There are some examples of algae that do not appear to assimilate NO₃⁻. Although not closely related to *B. bigelowii*, *Chrysochromulina breviturrita*, a freshwater haptophyte, cannot grow on NO₃⁻ as its sole N source, and is assumed to have a specialized N metabolism due to the acidic conditions where it lives [47]. The only other marine eukaryotic alga reported not to assimilate NO₃⁻ are mixotrophs from the family *Ochromonadaceae*, which acquire most of their required N by consuming prey and have potentially lost the genetic capability for NO₃⁻ assimilation and urea transport [48, 49].

It cannot be determined whether the lack of NO₃⁻ uptake results from genomic streamlining or metabolic control until genomes and/or transcriptomes from host cells are obtained. However, the observation that both haptophyte hosts do not assimilate NO₃⁻ suggests that the haptophyte's last common ancestor may not have relied on the assimilation of NO₃⁻ to meet their N demands prior to divergence [28]. Thus, N-acquisition strategies may be important in either establishing or maintaining symbioses between diazotrophs and eukaryotes, especially in the oligotrophic marine environment.

These experiments demonstrate that UCYN-A N₂ fixation supplies the needed N to support host cellular demands in both N-deplete and N-replete conditions. This is evident when comparing the C fixation rate to N transfer rate ratio (i.e., the ratio of the C fixation rate to the rate that N from UCYN-A N₂ fixation was transferred to the host cell) to the

best estimate of the UCYN-A/host symbiosis cellular C:N (6.3; [11]). In almost all instances the C fixation rate to N transfer rate ratio (Fig. 4a, c) was less than the cellular ratio, indicating that N₂ fixation met host N demands. In contrast, C fixation rates in UCYN-A2 were 32–75-fold greater than host NH₄⁺ uptake rates (Fig. 4d) indicating that NH₄⁺ uptake cannot solely meet haptophyte N demands. Thus, even in N-replete waters, N₂ fixation supported the UCYN-A1 and UCYN-A2 host requirements and NH₄⁺ uptake was a minor source of N for the symbiosis, despite it being energetically preferable [50, 51].

Notably, UCYN-A1 N₂ fixation could not fulfill the N required by the UCYN-A1 haptophyte host in NO₃.3 (C fixation rate to N transfer rate ratio greater than 6.3; Fig. 4b), suggesting the symbiosis requires exogenous N sources under some conditions. Potential N sources include dissolved organic N (DON) or acquiring N through mixotrophy. DON utilization by *E. huxleyi* has been demonstrated to be an important source of N in nutrient-depleted surface ocean waters [52, 53]. Phagotrophy may be unusual in some haptophyte lineages [54, 55]; however, haptophytes have also been identified as important grazers in coastal systems [56, 57]. UCYN-A haptophyte hosts have been identified as active predators of *Prochlorococcus* and *Synechococcus* in the North Pacific by Frias-Lopez et al. [58], although nothing was known about the symbiosis or the 18S rRNA gene sequences of the hosts at that time, so they were originally classified as unknown *Prymnesiophyceae*.

There are very few single-cell measurements of C and N transfer rates in the UCYN-A/haptophyte symbiosis, and those presented here are the first from associations living in coastally-influenced waters. Thus, we do not have a good understanding of the range or variability of these rates. Our rates are an order of magnitude greater than those reported by Krupke et al. [26]; however they used a C:N estimate for the UCYN-A/haptophyte symbiosis of 8.6, vs. while we applied a C:N of 6.3 as measured by [11] for our calculations. A higher C:N results in a lower per cell N content and thus lower absolute per cell N₂ fixation rates for an equal isotopic enrichment. While our transfer rates are higher than those reported by Krupke et al. [26], they are quite similar to the rates reported by Martinez-Perez et al. [11] from the subtropical N Atlantic for both UCYN-A1 and UCYN-A2 symbioses.

It was surprising that rate processes in the UCYN-A1/haptophyte symbiosis were at times enhanced by the addition of NO₃⁻ (Fig. 2d, l, Tables S15 and S19), given the lack of direct NO₃⁻ utilization (Fig. 2h). Phytoplankton and bacterioplankton are known to release dissolved substances, such as dissolved organic N, P, and C [59], B vitamins [60], and compounds that scavenge dissolved iron (e.g.,

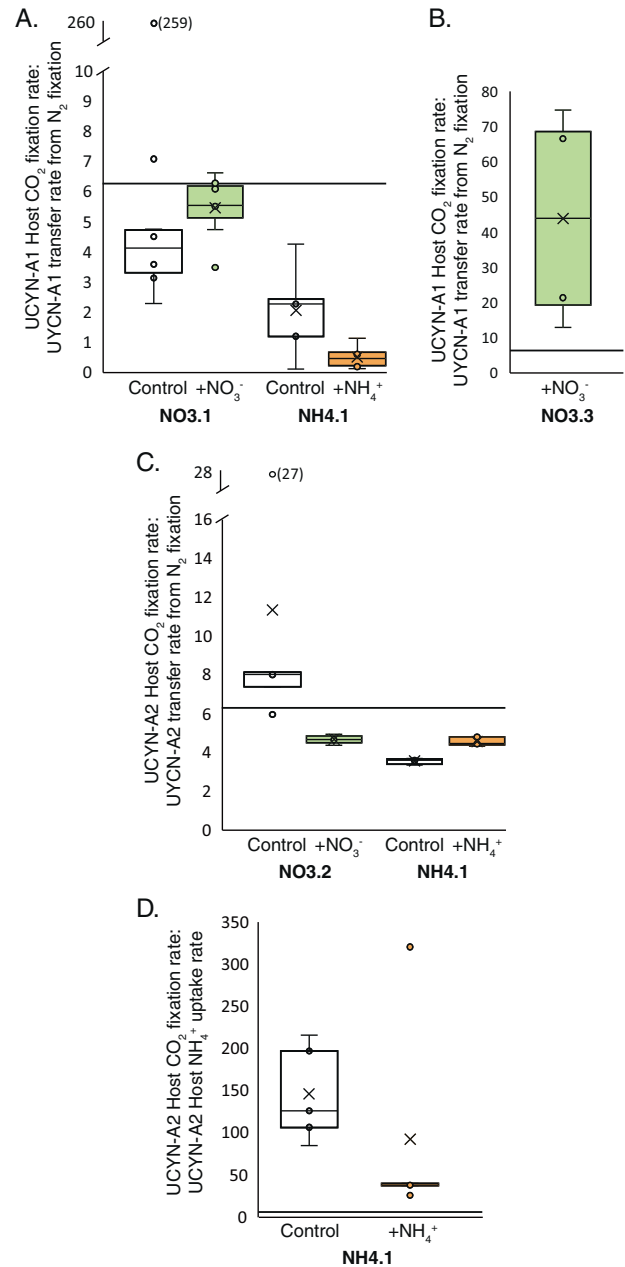


Fig. 4 N₂ fixation by UCYN-A supports the haptophyte host's N demands and cellular growth in DIN-deplete and DIN-replete waters. **a** Ratio of host CO₂ fixation rate to N transfer rate from N₂ fixation in the UCYN-A1/haptophyte symbiosis in NO₃.1 and NH₄.1. Note the break in y-axis. Mean value (30) for NO₃.1 control falls in break. **b** Ratio of host CO₂ fixation rate to N transfer rate from N₂ fixation in the UCYN-A1/haptophyte symbiosis in NO₃.3 NO₃⁻ treatment. **c** Ratio of host CO₂ fixation rate to N transfer rate from N₂ fixation in the UCYN-A2/haptophyte symbiosis in NO₃.2 and NH₄.1. **d** Ratio of host CO₂ fixation rate to NH₄⁺ uptake rate ratio in the UCYN-A2/haptophyte in NH₄.1. Cellular C:N ratio of 6.3 (solid line; [11]) is plotted on all graphs. Values that fall near or under the 6.3 ratio line indicate that cellular growth can be met by N₂ fixation. Data points that fall above the 6.3 ratio line indicate that cellular growth cannot be met by the N source.

siderophores, [61]), which have the potential to stimulate the fixation of CO₂ or N₂ by haptophytes and diazotrophs, respectively, even on these short time scales (<48 h; [62–64]). Vitamin B₁₂ is of particular interest, given that haptophytes are suspected to be B₁₂ auxotrophs [65]. The stimulating factor cannot be discerned from these experiments, nor whether CO₂ fixation by the haptophyte or N₂ fixation by the symbiont is directly stimulated. Further research is needed to identify the mechanism(s) of stimulation. However, experiments where the C fixation rate to N transfer rate ratio is less than the expected cellular C:N of 6.3 [11] demonstrate that an external C source may be required to meet cellular biomass demands (NO₃.1, NO₃.2, NH₄.1; Fig. 4a, c).

In conclusion, this is the first direct evidence that the UCYN-A/haptophyte symbiosis does not assimilate NO₃⁻, takes up little NH₄⁺ relative to N demands, and relies on N₂ fixation as its primary source of N in N-replete waters. These findings add to the growing body of evidence that N₂ fixation by one of the most widespread and important marine diazotrophs, the UCYN-A/haptophyte symbiosis, is not inhibited by DIN. However, the availability of DIN to the co-existing phytoplankton community may indirectly influence N₂ fixation and C fixation by the UCYN-A/haptophyte symbiosis. Current ecosystem and biogeochemical models predict little N₂ fixation in high latitude and temperate coastal regions [66, 67], contrary to recent reports of UCYN-A/haptophyte symbioses (and possibly other active diazotrophs) along with N₂ fixation in these regions [22, 68–70]. These insights into the biology of the UCYN-A/haptophyte symbioses may enable their inclusion in these models and improve our ability to predict the magnitude and distribution of N₂ fixation in environments previously considered unimportant with respect to diazotrophy.

Data and materials availability

All data are available in the main text or the supplementary materials.

Acknowledgements We gratefully acknowledge S. Spaugh, M. Kumar, J. Spakeen, C. Hakspiel, M. McPherson, B. Stewart, and M. Hogan for support processing samples in the field, and the captain and crew of the R/V Robert Gordon Sproul (SIO) for field logistical support. We also gratefully acknowledge D. Karl (UH Manoa) for providing access to the MIMS, M. R. Gradoville (UCSC) for helpful discussions on N₂ fixation rate calculations, and K. Negrey (UCSC), C. Gibble (UCSC), and R. Kudela (UCSC) for assistance with nutrient measurements. We gratefully acknowledge Clarissa Anderson and the SCCOOS monitoring program for providing access to nutrient data from the SIO Pier. Finally, we thank Farooq Azam (SIO) for providing us with laboratory and field support at the SIO pier. This work was supported by grants from the National Science Foundation (OCE-1559165 to JPZ and 1559152 to KRA and 1756524 to STW) and JPZ was also supported by grants from the Simons Collaboration on Ocean Processes and Ecology (SCOPE, grant 329108), and the Simons Foundation (grant 545171).

Author contributions MMM and KAT-K conceptualized the research and carried out formal analysis of the data; MMM, KAT-K, GLVD, BH, and KH performed field experiments; MIMS analysis was conducted by SW; funding acquisition and supervision were carried out by KRA and JPZ; the original draft was written by MMM and KT-K with input from JPZ, KRA, GLVD, SW, BH, and KH.

Compliance with ethical standards

Conflict of interest The authors declare that they have no conflict of interest.

Publisher's note Springer Nature remains neutral with regard to jurisdictional claims in published maps and institutional affiliations.

Open Access This article is licensed under a Creative Commons Attribution 4.0 International License, which permits use, sharing, adaptation, distribution and reproduction in any medium or format, as long as you give appropriate credit to the original author(s) and the source, provide a link to the Creative Commons license, and indicate if changes were made. The images or other third party material in this article are included in the article's Creative Commons license, unless indicated otherwise in a credit line to the material. If material is not included in the article's Creative Commons license and your intended use is not permitted by statutory regulation or exceeds the permitted use, you will need to obtain permission directly from the copyright holder. To view a copy of this license, visit <http://creativecommons.org/licenses/by/4.0/>.

References

- Moore CM, Mills MM, Arrigo KR, Berman-Frank I, Bopp L, Boyd PW, et al. Processes and patterns of oceanic nutrient limitation. *Nat Geosci.* 2013;6:701–10.
- Zehr JP, Ward BB. Nitrogen cycling in the ocean: new perspectives on processes and paradigms. *Appl Environ Microbiol.* 2002;68:1015–24.
- Capone D, Zehr J, Paerl H, Bergman B. *Trichodesmium*, a globally significant marine cyanobacterium. *Science.* 1997;276:1221–9.
- Villareal TA. Widespread occurrence of the hemiaulacynobacterial symbiosis in the southwest North-Atlantic Ocean. *Bull Mar Sci.* 1994;54:1–7.
- Zehr JP, Mellon MT, Zani S. New nitrogen fixing microorganisms detected in oligotrophic oceans by the amplification of nitrogenase (*nifH*) genes. *Appl Environ Microbiol.* 1998;64:3444–50.
- Thompson A, Carter BJ, Turk-Kubo K, Malfatti F, Azam F, Zehr JP. Genetic diversity of the unicellular nitrogen-fixing cyanobacteria UCYN-A and its prymnesiophyte host. *Environ Microbiol.* 2014;16:3238–49.
- Thompson AW, Foster RA, Krupke A, Carter BJ, Musat N, Vaulot D, et al. Unicellular cyanobacterium symbiotic with a single-celled eukaryotic alga. *Science.* 2012;337:1546–50.
- Tripp HJ, Bench SR, Turk KA, Foster RA, Desany BA, Niazi F, et al. Metabolic streamlining in an open-ocean nitrogen-fixing cyanobacterium. *Nature.* 2010;464:90–94.
- Bombar D, Heller P, Sanchez-Baracaldo P, Carter BJ, Zehr JP. Comparative genomics reveals surprising divergence of two closely related strains of uncultivated UCYN-A cyanobacteria. *ISME J.* 2014;8:2530–42.
- Cornejo-Castillo FM, Munoz-Marin MDC, Turk-Kubo KA, Royo-Llonch M, Farnelid H, Acinas SG, et al. UCYN-A3, a newly characterized open ocean sublineage of the symbiotic N₂

- fixing cyanobacterium candidatus *Atelocyanobacterium thalassa*. *Environ Microbiol.* 2019;21:111–24.
11. Martinez-Perez C, Mohr W, Loscher CR, Dekaezemaeker J, Littmann S, Yilmaz P, et al. The small unicellular diazotrophic symbiont, UCYN-A, is a key player in the marine nitrogen cycle. *Nat Microbiol.* 2016;1:16163.
 12. Postgate J. The origins of the unit of nitrogen fixation at the University of Sussex. *Notes Rec R Soc.* 1998;52:355–62.
 13. Knapp AN. The sensitivity of marine N₂ fixation to dissolved inorganic nitrogen. *Front Microbiol.* 2012;3:374.
 14. Holl CM, Montoya JP. Interactions between nitrate uptake and nitrogen fixation in continuous cultures of the marine diazotroph, *Trichodesmium* (cyanobacteria). *J Phycol.* 2005;41:1178–83.
 15. Mulholland MR, Capone DG. Nitrogen fixation, uptake, and metabolism in natural and cultured populations of *Trichodesmium* spp. *Mar Ecol Prog Ser.* 1999;188:33–49.
 16. Ohki K, Zehr JP, Falkowski PG, Fujita Y. Regulation of nitrogen-fixation by different nitrogen-sources in the marine non-heterocystous cyanobacterium *Trichodesmium* Sp Nibb1067. *Arch Microbiol.* 1991;156:335–7.
 17. Dekaezemaeker J, Bonnet S. Sensitivity of N₂ fixation to combined nitrogen forms (NO₃⁻ and NH₄⁺) in two strains of the marine diazotroph *Crocospaera watsonii* (cyanobacteria). *Mar Ecol Prog Ser.* 2011;438:33–46.
 18. Garcia NS, Hutchins DA. Light-limited growth rate modulates nitrate inhibition of dinitrogen fixation in the marine unicellular cyanobacterium *Crocospaera watsonii*. *PLoS ONE.* 2014;9:e114465.
 19. Großkopf T, Laroche J. Direct and indirect costs of dinitrogen fixation in *Crocospaera watsonii* WH8501 and possible implications for the nitrogen cycle. *Front Microbiol.* 2012;3:236.
 20. Bentzon-Tilia M, Traving SJ, Mantikci M, Knudsen-Leerbeck H, Hansen JLS, Markager S, et al. Significant N₂ fixation by heterotrophs, photoheterotrophs and heterocystous cyanobacteria in two temperate estuaries. *ISME J.* 2015;9:273–85.
 21. Shiozaki T, Fujiwara A, Ijichi M, Harada N, Nishino S, Nishi S, et al. Diazotroph community structure and the role of nitrogen fixation in the nitrogen cycle in the Chukchi Sea (western Arctic Ocean). *Limnol Oceanogr.* 2018;63:2191–205.
 22. Mulholland MR, Bernhardt PW, Blanco-Garcia JL, Mannino A, Hyde K, Mondragon E, et al. Rates of dinitrogen fixation and the abundance of diazotrophs in North American coastal waters between Cape Hatteras and Georges Bank. *Limnol Oceanogr.* 2012;57:1067–83.
 23. Mulholland MR, Bernhardt P, Widner B, Selden C, Chappell P, Clayton S, et al. High rates of N₂ fixation in temperate, western North Atlantic coastal waters expand the realm of marine diazotrophy. *Glob Biogeochem Cy.* 2019;33:826–40.
 24. Moreira-Coello V, Mouriño-Carballido B, Marañón E, Fernández-Carrera A, Bode A, Varela MM. Biological N₂ fixation in the upwelling region off NW Iberia: magnitude, relevance, and players. *Front Mar Sci.* 2017;4:303.
 25. Turk-Kubo KA, Connell PE, Caron DA, Hogan ME, Farnelid HM, Zehr JP. In situ diazotroph population dynamics under different resource ratios in the North Pacific Subtropical Gyre. *Front Microbiol.* 2018;9:1616.
 26. Krupke A, Mohr W, LaRoche J, Fuchs BM, Amann RI, Kuypers MM. The effect of nutrients on carbon and nitrogen fixation by the UCYN-A-haptophyte symbiosis. *ISME J.* 2015;9:1635–47.
 27. Cabello AM, Cornejo-Castillo FM, Raho N, Blasco D, Vidal M, Audic S, et al. Global distribution and vertical patterns of a prymnesiophyte-cyanobacteria obligate symbiosis. *ISME J.* 2016;10:693–706.
 28. Cornejo-Castillo FM, Cabello AM, Salazar G, Sanchez-Baracaldo P, Lima-Mendez G, Hingamp P, et al. Cyanobacterial symbionts diverged in the late Cretaceous towards lineage-specific nitrogen fixation factories in single-celled phytoplankton. *Nat Commun.* 2016;7:11071.
 29. Glibert PM and Capone DG. Mineralization and assimilation in aquatic, sediment, and wetland systems. In: Knowles R, Blackburn TH, editors. 'Nitrogen Isotope Techniques'. San Diego, CA: Academic Press; 1993, p. 243–72.
 30. Grasshoff K, Kremling K, Ehrhardt M, (eds). *Methods of Seawater Analysis.* Weinheim: Wiley-VCH; 1999. p. 600.
 31. Holm-Hansen O, Lorenzen CJ, Holmes RW, Strickland JD. Fluorometric determination of chlorophyll. *ICES J Mar Sci.* 1965;30:3–15.
 32. Mohr W, Großkopf T, Wallace DW, LaRoche J. Methodological underestimation of oceanic nitrogen fixation rates. *PLoS ONE.* 2010;5:e12583.
 33. Wilson ST, Böttjer D, Church MJ, Karl DM. Comparative assessment of nitrogen fixation methodologies, conducted in the oligotrophic North Pacific Ocean. *Appl Environ Microbiol.* 2012;78:6516–23.
 34. Böttjer D, Dore JE, Karl DM, Letelier RM, Mahaffey C, Wilson ST, et al. Temporal variability of nitrogen fixation and particulate nitrogen export at Station ALOHA. *Limnol Oceanogr.* 2017;62:200–16.
 35. Gradoville MR, Bombar D, Crump BC, Letelier RM, Zehr JP, White AE. Diversity and activity of nitrogen-fixing communities across ocean basins. *Limnol Oceanogr.* 2017;62:1895–909.
 36. Hernandez-de-la-Torre B, Gaxiola-Castro G, Alvarez-Borrego S, Gomez-Valdes J, Najera-Martinez S. Interannual variability of new production in the southern region of the California Current. *Deep Sea Res Part II-Topical Stud Oceanogr.* 2003;50:2423–30.
 37. Bronk D, Ward B. Inorganic and organic nitrogen cycling in the Southern California Bight. *Deep Sea Res Part I.* 2005;52:2285–300.
 38. Sigman DM, Karsh KL, Casciotti K. Nitrogen isotopes in the ocean, in *Encyclopedia of Ocean Sciences*, 2nd ed., J. H. Steele et al., editors. London: Academic; 2009. p. 40–54. <https://doi.org/10.1016/B978-012374473-9.00632-9>.
 39. Polerecky L, Adam B, Milucka J, Musat N, Vagner T, Kuypers MM. Look@ NanoSIMS—a tool for the analysis of nanoSIMS data in environmental microbiology. *Environ Microbiol.* 2012;14:1009–23.
 40. Kana TM, Darkangelo C, Hunt MD, Oldham JB, Bennett GE, Cornwell JC. Membrane inlet mass spectrometer for rapid high-precision determination of N₂, O₂, and Ar in environmental water samples. *Analytical Chemistry.* 1994;66:4166–70.
 41. Montoya JP, Voss M, Kahler P, Capone DG. A simple, high-precision, high-sensitivity tracer assay for N₂ fixation. *Appl Environ Microbiol.* 1996;62:986–93.
 42. Villareal TA. Laboratory culture and preliminary characterization of the nitrogen-fixing *Rhizosolenia-Richelia* symbiosis. *Mar Ecol.* 1990;11:117–32.
 43. Adam B, Klawonn I, Svedén JB, Bergkvist J, Nahar N, Walve J, et al. N₂-fixation, ammonium release and N-transfer to the microbial and classical food web within a plankton community. *ISME J.* 2016;10:450.
 44. Dortch Q, Clayton JR, Thoresen SS, Ahmed SI. Species-differences in accumulation of nitrogen pools in phytoplankton. *Mar Biol.* 1984;81:237–50.
 45. Bruhn A, LaRoche J, Richardson K. *Emiliania Huxleyi* (Prymnesiophyceae): nitrogen-metabolism genes and their expression in response to external nitrogen sources. *J Phycol.* 2010;46:266–77.
 46. Lindehoff E, Graneli E, Gilbert PM. Nitrogen uptake kinetics of *Prymnesium parvum* (Haptophyte). *Harmful Algae.* 2011;12:70–76.
 47. Wehr JD, Brown LM, O'Grady K. Highly specialized nitrogen metabolism in a freshwater phytoplankton, *Chrysochromulina breviturrita*. *Can J Fish Aquat Sci.* 1987;44:736–42.

48. Lie AA, Liu Z, Terrado R, Tatters AO, Heidelberg KB, Caron DA. Effect of light and prey availability on gene expression of the mixotrophic chrysophyte, *Ochromonas* sp. *BMC Genomics*. 2017;18:163.
49. Terrado R, Monier A, Edgar R, Lovejoy C. Diversity of nitrogen assimilation pathways among microbial photosynthetic eukaryotes. *J Phycol*. 2015;51:490–506.
50. Falkowski P. Enzymology of nitrogen assimilation. In: Carpenter EJ, Capone DG, ed. *Nitrogen in the Marine Environment*. NY: Academic Press; 1983.
51. Inomura K, Bragg J, Follows MJ. A quantitative analysis of the direct and indirect costs of nitrogen fixation: a model based on *Azotobacter vinelandii*. *ISME J*. 2017;11:166–75.
52. McKew BA, Metodjeva G, Raines CA, Metodiev MV, Geider RJ. Acclimation of *Emiliania huxleyi* (1516) to nutrient limitation involves precise modification of the proteome to scavenge alternative sources of N and P. *Environ Microbiol*. 2015;17:4050–62.
53. Palenik B, Henson SE. The use of amides and other organic nitrogen sources by the phytoplankton *Emiliania huxleyi*. *Limnol Oceanogr*. 1997;42:1544–51.
54. Dahl E, Bagøien E, Edvardsen B, Stenseth NC. The dynamics of *Chrysochromulina* species in the Skagerrak in relation to environmental conditions. *J Sea Res*. 2005;54:15–24.
55. Tillmann U. Phagotrophy by a plastidic haptophyte, *Prymnesium patelliferum*. *Aquat Micro Ecol*. 1998;14:155–60.
56. Chan Y-F, Chiang K-P, Ku Y, Gong G-C. Abiotic and biotic factors affecting the ingestion rates of mixotrophic nanoflagellates (Haptophyta). *Micro Ecol*. 2019;77:607–15.
57. Unrein F, Gasol JM, Not F, Forn I, Massana R. Mixotrophic haptophytes are key bacterial grazers in oligotrophic coastal waters. *ISME J*. 2014;8:164.
58. Frias-Lopez J, Thompson A, Waldbauer J, Chisholm SW. Use of stable isotope-labelled cells to identify active grazers of picocyanobacteria in ocean surface waters. *Environ Microbiol*. 2009;11:512–25.
59. Biddanda B, Benner R. Carbon, nitrogen, and carbohydrate fluxes during the production of particulate and dissolved organic matter by marine phytoplankton. *Limnol Oceanogr*. 1997;42:506–18.
60. Carlucci A, Bowes PM. Production of vitamin b12, thiamine, and biotin by phytoplankton 1. *J Phycol*. 1970;6:351–57.
61. Gledhill M, Buck KN. The organic complexation of iron in the marine environment: a review. *Front Microbiol*. 2012;3:69.
62. Smail, E. B-vitamins and trace metals in the Pacific Ocean: Ambient distribution and biological impacts. Los Angeles, California, USA: USC Digital Library, University of Southern California, University Park Campus MC 7002, 106 University Village; 2012.
63. Benavides M, Martias C, Elifantz H, Berman-Frank I, Dupouy C, Bonnet S. Dissolved organic matter influences N₂ fixation in the New Caledonian lagoon (Western Tropical South Pacific). *Front Mar Sci*. 2018;5:89.
64. Benavides M, Duhamel S, Van Wambeke F, Shoemaker KM, Moisaner PH, Salamon E, et al. Dissolved organic matter stimulates N₂ fixation and *nifH* gene expression in *Trichodesmium*. *FEMS Microbiol Lett*. 2020;367:fnaa034.
65. Nef C, Jung S, Mairet F, Kaas R, Grizeau D, Garnier M. How haptophytes microalgae mitigate vitamin B 12 limitation. *Sci Rep-Uk*. 2019;9:1–11.
66. Wang WL, Moore JK, Martiny AC, Primeau FW. Convergent estimates of marine nitrogen fixation. *Nature*. 2019;566:205–11.
67. Ward BA, Dutkiewicz S, Moore CM, Follows MJ. Iron, phosphorus, and nitrogen supply ratios define the biogeography of nitrogen fixation. *Limnol Oceanogr*. 2013;58:2059–75.
68. Fonseca-Batista D, Li X, Riou V, Michotey V, Deman F, Fripiat F, et al. Evidence of high N₂ fixation rates in the temperate northeast Atlantic. *Biogeosciences*. 2019;16:999–1017.
69. Harding K, Turk-Kubo KA, Sipler RE, Mills MM, Bronk DA, Zehr JP. Symbiotic unicellular cyanobacteria fix nitrogen in the Arctic Ocean. *Proc Natl Acad Sci USA*. 2018;115:13371–5.
70. Tang W, Wang S, Fonseca-Batista D, Dehairs F, Gifford S, Gonzalez AG, et al. Revisiting the distribution of oceanic N₂ fixation and estimating diazotrophic contribution to marine production. *Nat Commun*. 2019;10:831.